Electrochemical Oxidation of [1]Benzothieno[3,2-*b*]indole

Guiseppe Casalbore-Miceli, Giancarlo Beggiato, Salvatore S. Emmi, Alessandro Geri, and Benito Righetti
Istituto di Fotochimica e Radiazioni d'Alta Energia (FRAE) del Consiglio Nazionale delle Ricerche (C.N.R.), Via de' Castagnoli 1, I-40126 Bologna, Italy
Sergio Daolio
Istituto di Polarografia ed Elettrochimica Preparativa (IPELP) del Consiglio Nazionale delle Ricerche (C.N.R.), Corso Stati Uniti 4, I-35020 Padova, Italy

The oxidative behaviour of [1]benzothieno[3,2-*b*]indole (BTI) in methylene dichloride was investigated by an electrochemical technique. The process associated with the voltammetric wave at +1.04 V (*vs.* s.c.e.) leads to the protonated form of the BTI dimer. After slow deprotonation of this species the resulting dimer undergoes oxidation to give an oxidized dimer and, after a long electrolysis time, oxidized oligomers.

The electrochemical oxidation of heterocyclic molecules in organic media can lead to adducts with the solvent,[1] dimers,[2,3] and/or oxidized polymers.[4] The present paper reports part of an electrochemical study of heterocyclic aromatic molecules containing two different heteroatoms.

In a previous paper [5] the electrochemical behaviour of *N*-allyl-[1]benzothieno[3,2-*b*]indole (ABTI) † and the characteristics of the products obtained by its anodic oxidation were described. Electrolysis at the potential of the first oxidation wave (+1.3 V) in methylene dichloride gave no insoluble product; a black polymer film was deposited on the electrode at higher potentials.[6] The voltammetric and physicochemical characterization of this product is in progress.

A recent paper [4a] reports that anodic oxidation of a similar molecule, thieno[3,2-*b*]pyrrole (TP), at +0.6 V (*vs.* Ag/0.1N-$AgNO_3$) gave a conducting material (σ 5 × 10^{-3} ohm^{-1} cm^{-1}).

We discuss here the electrochemical oxidation of [1]benzothieno[3,2-*b*]indole † (BTI) at the potential of its anodic wave (+1.2 V *vs.* s.c.e.) in methylene dichloride. The behaviour of BTI is different from both that of ABTI in the same solvent and that of TP in acetonitrile.

Experimental

BTI was supplied by Ferrania S.p.A. and carefully purified by several techniques as reported for ABTI.[5] Methylene dichloride (Merck *pro analysi* and Aldrich Gold Label) was distilled over phosphorus pentaoxide under nitrogen. Tetrabutylammonium perchlorate (TBAP) (Fluka 'purum') was crystallized from methanol.

The electrochemical apparatus was a multifunction AMEL Electrochemolab instrument, connected to an AMEL 863 recorder. All the potentials are referred to a saturated calomel electrode (s.c.e.). Voltammetry was performed on deaerated samples with a Pt microelectrode. The electrolyses were done without deaeration, because no effect of oxygen was detected in these experiments. The working electrode was a platinum plate (1 cm^2). Other experimental details are reported in a previous paper.[5] All electrochemical measurements were carried out at room temperature (*ca.* 22 °C).

Pulse radiolysis experiments were carried out by means of the Linac accelerator facilities described elsewhere.[7]

Mass spectra were obtained with a double-focusing VG ZAB 2F spectrometer operating in the electron impact mode (70 eV; 200 A) with a source temperature of 200 °C.

† ABTI and BTI have been previously referred to as *N*-allyl-thionaphthene-indole (ATNI) and thionaphthene-indole (TNI), respectively.

Results

Diffusion-layer renew voltammetry (d.l.r.v.) of *ca.* 10^{-3}M-BTI in methylene dichloride [Figure 1(a)] shows an anodic wave A, with $E_{\frac{1}{2}}$ +1.04 V, followed by a small wave B, with $E_{\frac{1}{2}}$ 1.20 V. Because these waves are close to each other, a small uncertainty is associated with their quoted half-wave potentials.

The ratio between the limiting currents of waves B and A, $i_{l(B)}/i_{l(A)}$, increases with increasing concentration of BTI, being 0.06 for [TNI] = 0.48 × 10^{-3}M and 0.31 for [TNI] = 4.53 × 10^{-3}M.

For wave A, the plot of potential E *versus* $\lg[(i_l - i)^2/i]$ deviates from linearity, with an average slope of about 37 mV.

Cyclic voltammetry (c.v.) of *ca.* 10^{-3}M-BTI [Figure 2(a)] presents an anodic peak α at +1.12 V, with the corresponding cathodic peak β at +0.98 V, a small peak γ at +0.26 V, and a peak δ at −0.3 V (sweep rate v = 100 mV s^{-1}). At lower rates (50 and 20 mV s^{-1}), a small anodic peak α' at +1.24 V and the corresponding cathodic peak β' at +1.16 V are observed. On increasing the BTI concentration beyond 10^{-3}M, peak α' becomes detectable at 50 mV s^{-1}. The value of $i_{p(\alpha)}/v^{\frac{1}{2}}$, where $i_{p(\alpha)}$ is the peak current, decreases slightly with increasing v in the range 500—1 000 mV s^{-1}. The value of $i_{p(\beta)}/i_{p(\alpha)}$ increases with increasing v for a given BTI concentration. At a given sweep rate, this ratio decreases on increasing the concentration (Table).

Inexhaustive electrolyses were carried out at +1.2 V, for [TNI] *ca.* 10^{-3}M, with an average electron consumption per molecule as high as 1.55. This value was calculated from the ratio between the heights of wave A before and after electrolysis; the height was found to be proportional to [BTI] in our experimental range (0.5 × 10^{-3} to 4.4 × 10^{-3}M). The number of electrons per molecule of monomer increases with the progress of the electrolysis. After electrolysis, two cathodic waves, C at *ca.* +0.3 V and D at *ca.* −0.2 V, appear [Figure 1(b)]. Wave C can appear split, and its half-wave potential changes (+0.22 to +0.35 V), depending on the progress of electrolysis and on the monomer concentration.

On electrolysing *ca.* 10^{-3}M-BTI no solid product was found. With higher concentrations of BTI ($\geq 2 \times 10^{-3}$M), the consumption of electrons per molecule increases, approaching two when the current is about 10% of its initial value. The residual current persists over several days, while a thin black layer begins to appear on the electrode.

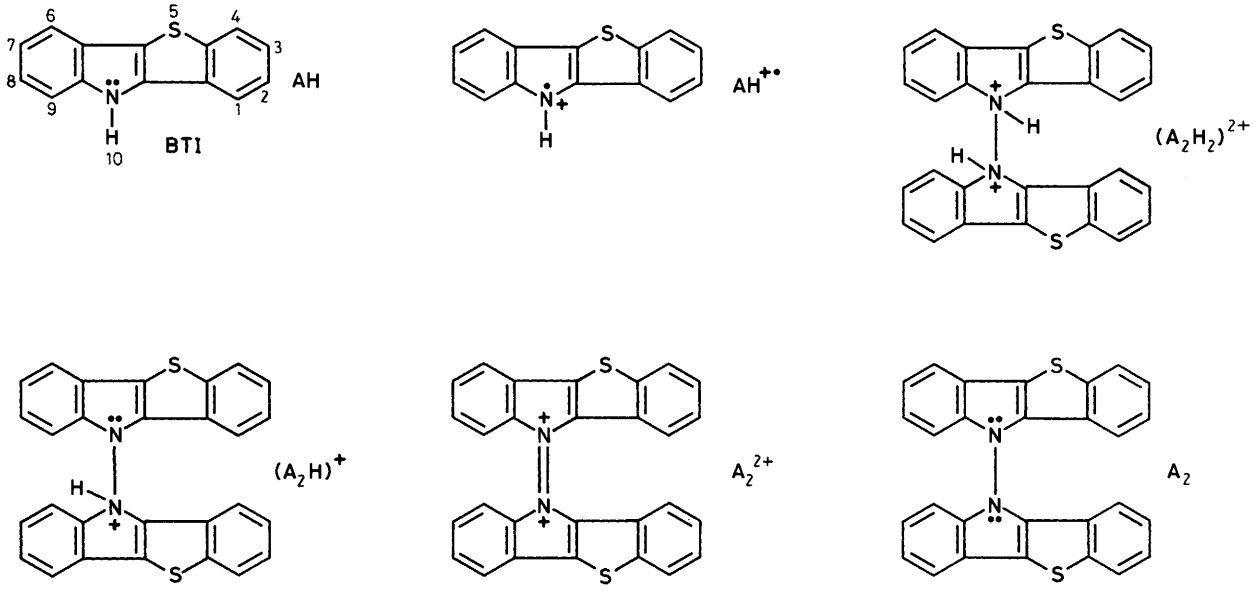

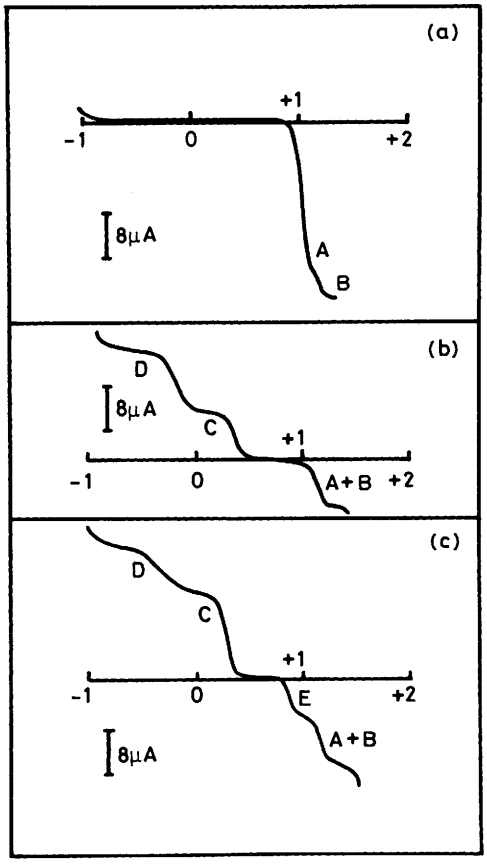

Figure 1. (a) D.l.r.v. of 1.43×10^{-3}M-BTI in methylene-chloride (supporting electrolyte 0.1M-TBAP); (b) d.l.r.v. of 1.36×10^{-3}M-BTI in methylene dichloride (supporting electrolyte 0.1M-TBAP) immediately after electrolysis at +1.2 V (after the flow of 5.6 coulombs); (c) d.l.r.v. of the same solution as (b) about 24 h after the electrolysis

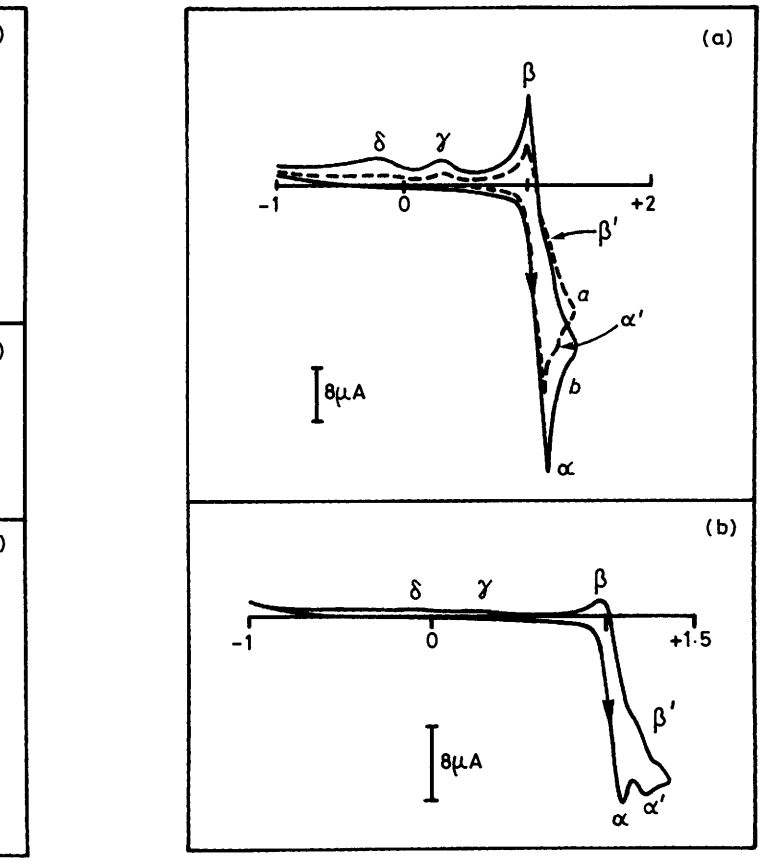

Figure 2. (a) C.v. of 1.13×10^{-3}M-BTI in methylene dichloride (supporting electrolyte 0.1M-TBAP) at (*b*) 100 mV s^{-1} (*a*) 50 mV s^{-1}; (b) as (a), at 20 mV s^{-1}

Logarithmic analysis of wave C gives a slope of 81 mV for the plot of potential *E versus* $\lg[(i_l - i)/i]$; that of wave D gives a slope of 125 mV for the same plot.

C.v. after electrolysis [Figure 3(a)] shows a residual anodic peak *a* at +1.22 V and the corresponding peak *b* at +1.10 V, preceded by a small anodic peak *c* at +0.94 V and a cathodic peak *d* at +0.82 V.

The cathodic peaks *e*, at +0.35 V, and *f*, at −0.15 V, are much higher than peaks γ and δ before electrolysis. The peak potentials (E_p) of *e* and *f* undergo an anodic shift on increasing

Table. Values of $i_{p(\beta)}/i_{p(\alpha)}$ for different BTI concentrations and sweep rates (sweep range −1 to +1.5 to −1 V)

	Sweep rate (mV s^{-1})					
10^3[TNI]/M	20	50	100	200	500	1 000
0.48		0.24	0.36			
0.96	0.07	0.21	0.30			
1.14			0.24	0.34	0.46	0.65
1.44	0.05	0.15	0.24			
1.92	0.04	0.15	0.21			
2.25			0.17	0.24	0.38	
4.53			0.13	0.19	0.29	0.32

the sweep rate: for *f*, E_p goes from −0.24 V for 20 mV s^{-1} to −0.10 V for 200 mV s^{-1}; for *e*, E_p goes from +0.28 V for 20 mV s^{-1} to +0.40 V for 200 mV s^{-1}. The value of $i_p/v^{\frac{1}{2}}$ decreases, with increasing *v*, from 1.25 (i_p in μA) for v = 20 mV s^{-1} to 0.23 for v = 200 mV s^{-1} for peak *e*, and from 1.16 (20 mV s^{-1}) to 0.84 (100 mV s^{-1}) for peak *f*.

Peak *f* shows a characteristic sigmoid shape, especially evident at low sweep rates.

The voltammetric pattern of the electrolysed system changes markedly with time. In d.l.r.v. [Figure 1(c)] a decrease of wave D and an increase of wave C were observed. Wave C shifts towards cathodic potentials ($\Delta E_{\frac{1}{4}}$ 90—100 mV) and the slope of the plot of potential *E versus* lg[$(i_l - i)/i$] decreases from about 80 to 70—74 mV. A new anodic wave E appears at +0.88 V {slope of the plot of potential *E versus* lg[$(i_l - i)/i$] = 40—45 mV}, while i_l of wave A does not change.

In c.v. [Figure 3(b)] analogous variations were seen. Peak *f* decreases and peak *e* increases. Peak *c*, at +0.91 V, and the corresponding cathodic peak *d*, at +0.88 V, undergo a marked increase; they have almost the same i_p value [$i_{p(d)}$ is slightly smaller than $i_{p(c)}$] and neither E_p nor $i_p/v^{\frac{1}{2}}$ depends on *v* in the range 50—200 mV s^{-1}.

On electrolysing solutions of BTI more concentrated than 2×10^{-3}M, the voltammetric pattern undergoes minor changes with time after electrolysis. Just after anodic electrolysis at +1.2 V, a cathodic electrolysis was carried out at the plateau potential of the cathodic wave C (+0.05 V): wave E appeared suddenly, with a concomitant decrease of waves C and D [Figure 4(a)]. Analogous changes were observed in c.v. [Figure 4(b)].

At this stage the electrolysed sample were analysed by mass spectrometry. Good mass spectra were obtained with difficulty, owing to the presence of TBAP. However, peaks corresponding to the molecular weight of the dimer (*m*/*z* 444) and as expected for its fragmentation were present; some other peaks at higher masses and with very low relative abundances revealed the presence of minor amounts of oligomers.

The u.v.–visible spectrum of BTI [Figure 5(b)] shows two systems of bands, in the regions 230—260 (ε_{252} 23 000 dm^3 mol^{-1} cm^{-1}) and 310—314 (ε_{313} 20 400 dm^3 mol^{-1} cm^{-1}), with a shoulder at 332 nm (ε_{332} 9 900 dm^3 mol^{-1} cm^{-1}). After electrolysis of *ca.* 10^{-3}M-BTI at +1.2 V, these systems of bands appeared less intense and less structured [Figure 5(b)]. A shoulder at 360—380 nm and two new bands in the visible region appeared: the former, with $\lambda_{max.}$ 517 nm, had a shoulder at 477 nm; the latter was very broad, with the maximum at 685 nm. For higher concentrations ([TNI] ≥ 2×10^{-3}M), the spectrum after electrolysis approaches that of ABTI under the same experimental conditions (attributed to the dimer dication),[5] with two visible bands at 529 (with no shoulder) and 681 nm, with intensity ratio *ca.* 2:1 [inset Figure 5(b)]. Just after the electrolysis the visible bands slowly decreased, but their shape remained almost unaltered. The u.v. part of the spectrum shows marked changes only for low concentrations of BTI. Figure 5(c) shows the spectrum recorded 24 h later, which corresponds to the voltammetric pattern of Figure 1(c). The spectrum after a partial cathodic electrolysis on wave C shows a decrease of the bands in the visible region, while, as mentioned before, wave E increases and waves C and D decrease.

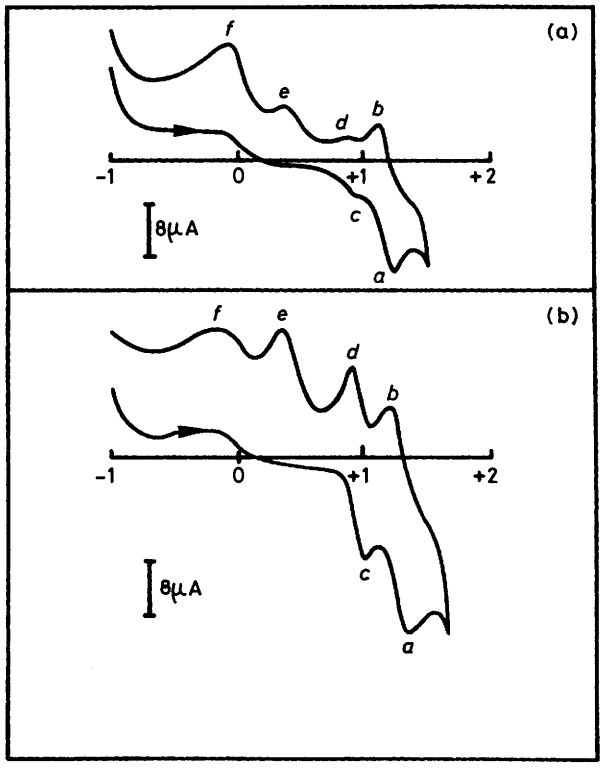

Figure 3. (a) C.v. of 1.36×10^{-3}M-BTI in methylene dichloride (supporting electrolyte 0.1M-TBAP) immediately after electrolysis at +1.2 V (after the flow of 5.6 coulombs); scan rate 100 mV s^{-1}; (b) c.v. of the same as (a), about 24 h after the electrolysis

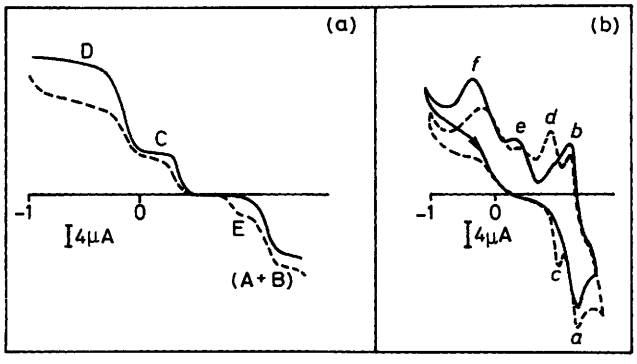

Figure 4. (a) D.l.r.v. of 1.21×10^{-3}M-BTI in methylene dichloride (supporting electrolyte 0.1M-TBAP), after electrolysis at +1.2 V (after the flow of 5.32 coulombs; initial current 0.7 mA; final current 0.19 mA, nearly constant) (full line) and after a subsequent electrolysis at −0.05 V (after the flow of 0.28 coulombs; initial current 0.4 mA; final current 0.05 mA, nearly constant) (dashed line); (b) c.v. corresponding to the d.l.r.v. of (a), after electrolysis at +1.2 V (full line) and after a subsequent electrolysis at −0.05 V (dashed line)

$$AH \underset{}{\overset{-e}{\rightleftharpoons}} AH^{+\cdot} \quad (1)$$

$$2AH^{+\cdot} \longrightarrow (A_2H_2)^{2+} \quad (2)$$

$$2AH^{+\cdot} \xrightarrow[-2e]{-2H^+} A_2^{2+} \text{ (for 7,7'-coupling)} \quad (2')$$

$$(A_2H_2)^{2+} \rightleftharpoons (A_2H)^+ + H^+ \quad (3)$$

$$(A_2H)^+ \rightleftharpoons A_2 + H^+ \quad (4)$$

$$(A_2H)^+ \overset{-e}{\rightleftharpoons} (A_2H)^{2+\cdot} \xrightarrow[-e]{-H^+} A_2^{2+} \quad (5)$$

$$A_2 \xrightarrow{-2e} A_2^{2+} \quad (6)$$

$$AH^{+\cdot} + A_2^{2+} \longrightarrow T^{+\cdot} + 2H^+ \longrightarrow \cdots P^{+\cdot} \quad (7)$$

Scheme. Proposed mechanism for 10,10'-coupling

N.B. Equation (2') is here inserted for the sake of completeness. In all the equations reported, AH stands for BTI, T for trimer, and P for polymer.

Discussion

The behaviour of BTI, when oxidized on the plateau of the overall anodic wave (A + B), is rather different from that of ABTI oxidized on the corresponding waves, as shown by the consumption of electrons, which in the case of low concentrations of BTI is intermediate between one and two per molecule.

On oxidation of BTI at +1.2 V, the suggested mechanism (Scheme) involves the formation of a cation radical, which subsequently dimerizes by coupling at various positions.

For ABTI, position 7 was identified as the most probable coupling site,[5] because position 9 is sterically hindered and position 10 is unavailable, but for BTI, by comparison with similar heterocyclic molecules,[8,9] one of the most reactive positions could be the nitrogen atom (position 10). This fact is probably responsible for the different behaviour of ABTI and BTI with respect to oxidation. In particular, the different consumption of electrons, in certain conditions less than two per molecule for BTI, suggests a mechanism where, after an oxidation step, the radical cations dimerize mainly at position 10, with formation of quaternary nitrogen structures and a subsequent acid–base equilibrium and/or slow release of protons. An example of slow deprotonation, following coupling between cation radicals produced by an electrochemical technique, is reported in ref. 10. This deprotonation should not greatly influence the electrode kinetics, but it would increase the consumption of electrons during the electrolysis, because the deprotonated 10,10'-dimer could be further oxidized on the electrode. A concomitant minor 7,7'-coupling, as for ABTI,[5] should be followed by a faster deprotonation and oxidation of the dimer with an overall bielectronic mechanism. All this is supported by several experimental observations, which will be discussed in detail.

The anodic wave A seems to be monoelectronic; in fact, for this wave, the height of which is proportional to the concentration of BTI, the slope of the plot of potential *E versus* $\lg[(i_l - i)/i]$ is 60 mV. The plot of *E versus* $\lg[(i_l - i)^2/i]$ does not agree perfectly with a monoelectronic process followed by a fast dimerization. In any case, since the consumption of electrons per molecule is less than two, a bielectronic irreversible process is improbable, at least for low concentrations. However, for the peak α, the value of $i_p/v^{\frac{1}{2}}$ as for ABTI, slightly decreases, while $i_{p(\beta)}/i_{p(\alpha)}$, where β is the reduction peak corresponding to the anodic peak α, increases with increasing sweep rate. This clearly suggests kinetic behaviour which follows the first electronic transfer (formation of radical monocation). Probably the rate constant of the subsequent dimerization of the radical cation does not meaningfully influence the logarithmic plot for wave. A. The shape of the wave might also be influenced by several compensatory factors, such as an electron transfer which is not fully reversible, cell resistance, cation radicals adsorbed on the electrode, *etc.*

On the other hand, wave B, subsequent to the monoelectronic wave A, can account for other steps which follow the dimerization. Indeed, dimerization at position 10 (the most probable coupling site) could give, by a monoelectronic process, a rather stable diprotonated dimer $(A_2H_2)^{2+}$. The relative stability of $(A_2H_2)^{2+}$, in contrast to the case of ABTI, is also shown by c.v. of the monomer (AH) (Figure 2), where peaks *c* and *d*, associated with the redox process of the dimer (A_2), are missing. These peaks appear after electrolysis at +1.2 V (Figure 3), when reactions (3) and (4) have time to occur. The dimer $(A_2H_2)^{2+}$, however, could be involved in fast acid–base equilibration at the electrode–solution interface, with formation of a monoprotonated dimer, the oxidation of which should be responsible for peak α' [Scheme, step (5)].

In conclusion, the alternative 7,7'-coupling, which, as for ABTI, leads to an overall bielectronic (e.c.c.e.)* process, where the two electron transfers are separated by the two fast reactions of coupling and deprotonation, seems to be, in the case of BTI, a very minor reaction, at least as long as position 10 is free to react. In this connection, it must be remembered that wave A appears to be monoelectronic and that the electron consumption on electrolysis of BTI solutions of low concentration is less than two per molecule.

The mechanism proposed for BTI, which associates the peaks α, α', β, and β' with the steps (1), (2), (3), and (5) of the Scheme, is supported by the following observations.

(i) The value of $i_{p(\beta)}/i_{p(\alpha)}$ increases with increasing *v*: this accounts for the reduction of a greater amount of BTI radical cation ($AH^{+\cdot}$) at high sweep rates, because under these conditions the radicals have less time to dimerize.

(ii) The value of $i_{p(\beta)}/i_{p(\alpha)}$ decreases with increasing [BTI]: in fact, high [BTI] means high $i_{p(\alpha)}$, *i.e.* high [$AH^{+\cdot}$] on the electrode, which implies a high rate of radical coupling.

(iii) The same arguments explain the increase of $i_{p(\alpha')}/i_{p(\alpha)}$ with increasing [BTI]. Moreover, the increase of this expression, as well as of $i_{l(B)}/i_{l(A)}$, with increasing [BTI] might be also due to an acid–base equilibrium (3') involving BTI.

$$(A_2H_2)^{2+} + AH \rightleftharpoons (A_2H)^+ + (AH_2)^+ \quad (3')$$

In this respect, it must be pointed out that, in voltrammetry of BTI electrolysed at +1.2 V, $i_{p(\alpha')}/i_{p(\alpha)}$ and $i_{l(B)}/i_{l(A)}$ increase with the extent of electrolysis; after the flow of 1.5—1.7 electrons per molecule, only a small wave B and a correspondingly small peak α' are present. This is probably due to the increasing ratio between protonated and unprotonated species in solution. In any case, in voltammetry of non-electrolysed BTI, $i_{p(\alpha')}/i_{p(\alpha)}$ remains very small even though $i_{p(B)}$ is markedly lowered with respect to $i_{p(\alpha)}$: this further supported the hypothesis of an e.c.c.e. sequence [Scheme, steps (1), (2), (3), and (5)], where, after the electron transfer responsible for peak α [step (1)] and the subsequent kinetics [step (2)], a further chemical process [step (3)] leading to the electroactive species associated with peak α' [step (5)], is suggested.

During the electrolysis of [BTI] $\geqslant 2 \times 10^{-3}$M, the enhanced coupling rate due to the increase in concentration and the corresponding shift to the right of all the equilibria [Scheme, steps (2) and (5)] force the system towards formation of the dimer dication $(A_2H_2)^{2+}$ and of the products of the subsequent steps, while oligomers are formed by coupling of oxidized

* E.c.c.e = electrochemical-chemical-chemical-electrochemical.

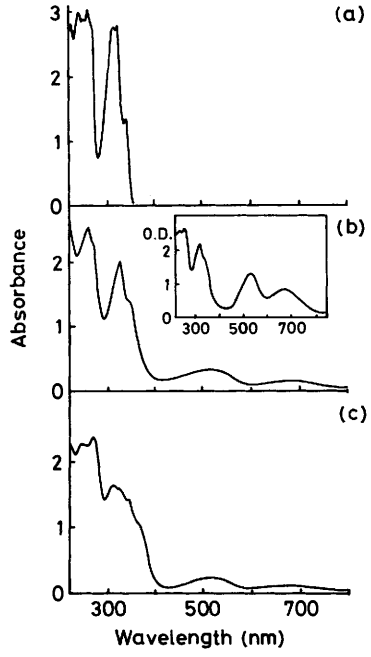

Figure 5. U.v.–visible spectra of (a) 1.36×10^{-3}M-BTI in methylene dichloride (supporting electrolyte 0.1M-TBAP); (b) 1.36×10^{-3}M-BTI in methylene dichloride (supporting electrolyte 0.1M-TBAP) after electrolysis at +1.2 V (flow of 5.6 coulombs); (c) the same solution as (b), about 24 h after the electrolysis. *Inset:* Qualitative u.v.–visible spectrum of [BTI] $\geqslant 2 \times 10^{-3}$M in methylene dichloride (supporting electrolyte 0.1M-TBAP) after electrolysis at +1.2 V (for all spectra optical path 0.1 cm)

molecules on the electrode [*e.g.* Scheme, step (7)]. This is confirmed by the mass spectra of the products of the system electrolysed at the potential of wave C.

The voltammetric pattern, after electrolysis at +1.2 V, changes with time, showing a decrease of the cathodic wave D almost equivalent to the increase of the anodic wave E at +0.88 V [it is to be noted that, at almost the same potential (+0.9 V), ABTI presents an anodic wave attributed to oxidation of the dimer] and the increase of the cathodic wave C, $E_{\frac{1}{4}}$ of which tends to more negative values.

For ABTI, a wave at +0.38 V was attributed to an adduct between the oxidized dimer and $HClO_4$ and considered to be indistinguishable from the reduction wave of free $HClO_4$ in methylene dichloride, which occurs at more negative potential, but not so different as to cause a distinct wave with respect to the adduct (for $[HClO_4] = 4.7 \times 10^{-3}$M, $E_{\frac{1}{4}} = +0.22$ V).[5] The same interpretation can be given for wave C of electrolysed BTI ($E_{\frac{1}{4}} = +0.35$ V). However, during the electrolysis of BTI at + 1.2 V, an inflection of this wave can be observed, depending on the relative amounts of the species in solution: this is in accord with the foregoing hypothesis.

The cathodic waves C and D are explained by the following mechanism. For wave C and peak γ, as already suggested for ABTI, the processes (8) and (9) (not easily distinguishable) are

$$(A_2^{2+}\cdot 2ClO_4^-)\cdot 2HClO_4 \xrightarrow{+2e} A_2 + 2ClO_4^- + 2HClO_4 \quad (8)$$

$$2HClO_4 \xrightarrow{+2e} H_2 + 2ClO_4^- \quad (9)$$

proposed. The oxidized dimer A_2^{2+} can be produced by a coupling process followed by deprotonation and oxidation during electrolysis at +1.2 V.

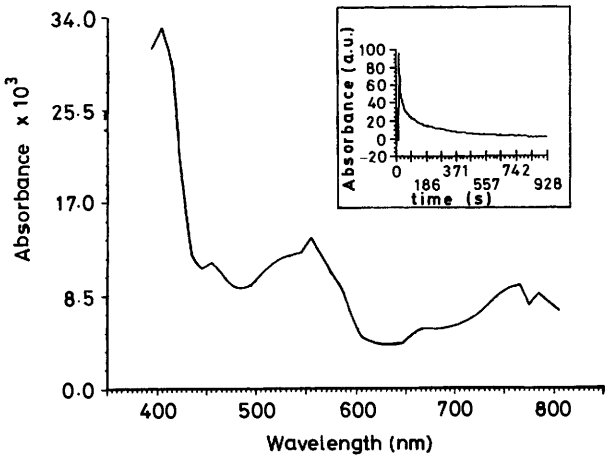

Figure 6. Transient spectrum obtained on pulse radiolysis of 3.3×10^{-4}M-BTI in deaerated methylene dichloride; pulse length 100 ns, dose normalized to 7 krad, optical path 2 cm, time after the start of the pulse 1.2 μs. *Inset:* Typical optical trace showing that the visible absorption of $BTI^{+\cdot}$ disappears almost completely in about 1 ms (λ 560 nm, optical path 2 cm, dose about 14 krad, pulse length 100 ns)

For this process, the c.v. measurements agree with the preceding kinetics and therefore with a mechanism such as (10)

$$(A_2^{2+}\cdot 2ClO_4^-)\cdot 2HClO_4 \rightleftharpoons 2HClO_4 + (A_2^{2+}\cdot 2ClO_4^-) \quad (10)$$

and (11). In any case, the overlap of the processes connected

$$(A_2^{2+}\cdot 2ClO_4^-) \xrightarrow{+2e} A_2 + 2ClO_4^- \quad (11)$$

with the reductions of the adduct and of $HClO_4$ makes peak γ and wave C difficult to interpret.

The reasoning produced for ABTI,[5] as well as the following arguments, confirms that wave C does not pertain solely to the reduction of free $HClO_4^-$ [reaction (9)].

(*a*) Free $HClO_4$, during electrolysis at +1.2 V, must be produced simultaneously with the oxidized dimer A_2^{2+} [Scheme, steps (1)—(4) and (6)]. This species, free, has a reduction potential of about +0.8 V (see c.v. of BTI, peak *d*). Therefore it seems improbable that it is reduced at a potential more negative than −1 V.

(*b*) After the total disappearance of wave D, wave C decreases slowly, contemporaneously with a decrease of the 'visible' absorbance, which was attributed to the cationic species produced by BTI oxidation.

Wave D and the corresponding peak *f* can be associated with a reduction process (12) involving the protonated dimer. This

$$(A_2H_2)^{2+} \xrightarrow{+2e} A_2 + H_2 \quad (12)$$

can also explain a decrease of wave D, due to a shift to the right of reaction (13), besides the decrease of wave C and the

$$(A_2H_2)^{2+} + 2ClO_4^- \longrightarrow A_2 + 2HClO_4 \quad (13)$$

appearance of wave E, when the system is electrolysed at the potential of wave C. In fact, the observed decrease of wave D can be associated with the thermal process (13). This process also explains the parallel increase of wave C (formation of $HClO_4$) and the concomitant growth of wave E (production of A_2); this latter wave, as well as the corresponding peaks *c* and *d* [Figures 1(b) and (c), and 3(a) and (b)] can be associated with the redox reactions of the dimer A_2 [Scheme, step (6)].

The association of wave E with oxidation of A_2 is supported by the increase of the 'visible' bands and of wave C observed after electrolysis on the plateau of this wave at +1 V. Moreover, as already mentioned, in the case of ABTI an anodic wave at about the same potential as wave E of BTI was also attributed to the oxidation of the corresponding dimer.[5]

For ABTI,[5] after exhaustive electrolysis, when an equivalent amount of dioxidized 7,7′-dimer had been produced, the spectrum showed two bands, ascribed to the dimer dication, with ε_{531} 28 000 and ε_{701} 14 000 $dm^3\ mol^{-1}\ cm^{-1}$. In the case of *ca.* 10^{-3}M-BTI, two low-intensity bands with $\lambda_{max.}$ 480 and 685 nm were observed. However, in this case the extinction coefficients could not be evaluated, because the spectral contributions of the two species present, *i.e.* the oxidized dimers A_2^{2+} and $(A_2H_2)^{2+}$, are not known.

The BTI[11a] and ABTI[11b] radical monocations ($AH^{+\bullet}$) were also produced by pulse radiolysis in the same medium and their transient spectra were recorded as a function of time. Their characteristic bands, appearing around 550 and 750 nm (Figure 6), decay rapidly with first-order kinetics, after which no absorption in the visible region is left (inset, Figure 6). This bleaching process has been interpreted as the release of the proton linked to nitrogen.[11a] By comparing the spectra of Figures 5(b) and 6, the pulse radiolysis measurements lead to the conclusion that the electrolysis product, absorbing in the visible, does not come from an interaction between the solvent and the radical cation itself; it is due, instead, to an oxidized species derived from a dimerization process on the electrode.

The spectral variations observed mainly in the u.v. region after electrolysis at +1.2 V of solutions of low concentration [Figure 5(c)], as well as the parallel voltammetric changes, might be due to deprotonation of $(A_2H_2)^{2+}$. Moreover, the fact that the spectra of [BTI] $\geqslant 2 \times 10^{-3}$M and ABTI approach each other when they are electrolysed under the same experimental conditions, and do not undergo variation with time, agrees with the mechanism proposed. In fact, higher concentrations of BTI, driving the equilibria involved to the right, favour the final production of a greater amount of A_2^{2+} and higher homologues.

Conclusions

The results of the electrochemical oxidation of BTI at +1.2 V differ from those obtained with ABTI, in the same range of working potentials.

Radical cations of BTI can undergo a 10,10′-coupling reaction which for ABTI is sterically hindered by the allyl group. Moreover the oxidation process of ABTI is bielectronic, with probable 7,7′-coupling; for BTI, the consumption of electrons, for the same process on the corresponding voltammetric wave, was found to be between one and two per molecule, owing to the slowness of the deprotonation following the 10,10′-coupling reaction between two radical cations.

Oligomers can also be produced, provided that BTI solutions of relatively high concentration are electrolysed at +1.2 V for a long time, which favours deprotonation of the dimer.

Acknowledgements

We thank Mr. B. Facchin for mass spectrometric measurements and Mr. G. Gubellini for drawing the Figures.

References

1 R. J. Waltman, A. F. Diaz, and J. Bargon, *J. Phys. Chem.*, 1984, **88**, 4343.
2 M. Genies and A. F. Diaz, *J. Electroanal. Chem.*, 1979, **98**, 305.
3 A. Desbene-Monvernay, P. C. Lacaze, and J. E. Dubois, *J. Electroanal. Chem.*, 1981, **129**, 229.
4 For papers dealing with polymerization of molecules containing two different heteroatoms see (*a*) R. Lazzaroni, J. Riga, J. J. Verbist, L. Christiaens, and M. Renson, *J. Chem. Soc., Chem. Commun.*, 1985, 999; (*b*) G. Mengoli, M. M. Musiani, and G. Zotti, *J. Electroanal. Chem.*, 1984, **175**, 93; (*c*) G. G. McLeod, M. G. B. Mahboubian-Jones, R. A. Pethrick, S. D. Watson, N. D. Truong, J. C. Galin, and F. Francois, *Polymer*, 1986, **27**, 455; (*d*) S. Naitoh, K. Sanui, and N. Ogata, *J. Chem. Soc., Chem. Commun.*, 1986, 1348; (*e*) M. Aldissi, D. Wrobleski, and S. Gottfield, *Polym. Mater. Sci. Eng.*, 1986, **55**, 730; (*f*) M. Chandrasekaran and V. Krishnan, *Trans. SAEST*, 1986, **21**, 25.
5 G. Casalbore-Miceli, G. Beggiato, S. Daolio, P. G. Di Marco, S. S. Emmi, and G. Giro, *Ann. Chim. (Rome)*, 1987, **77**, 609.
6 G. Casalbore-Miceli, G. Beggiato, P. G. Di Marco, S. S. Emmi, G. Giro, and B. Righetti, *Synth. Met.*, 1986, **15**, 1.
7 S. S. Emmi, G. Beggiato, and G. Casalbore-Miceli, *Radiat. Phys. Chem.*, submitted.
8 J. F. Ambrose and R. F. Nelson, *J. Electrochem. Soc.*, 1968, **115**, 1161.
9 R. J. Waltman and J. Bargon, *Can. J. Chem.*, 1986, **64**, 76.
10 C. Berti, L. Greci, R. Andruzzi, and A. Trazza, *J. Org. Chem.*, 1985, **50**, 368.
11 S. S. Emmi, G. Beggiato, and G. Casalbore-Miceli, (*a*) 'Proc. 6th Tihany Symp. Radiat. Chem., Akademiai Kiado,' Budapest, 1987, 363; (*b*) unpublished results.

Received 19*th June* 1987; *Paper* 7/1091